Einstein-Podolsky-Rosen steering in spontaneous parametric down-conversion cascaded with a sum-frequency generation

Y. Liu, S. L. Liang, G. R. Jin, Y. B. Yu,* and A. X. Chen†
Key Laboratory of Optical Field Manipulation of Zhejiang Province, Department of Physics, Zhejiang Sci-Tech University, Hangzhou 310018, China

(Received 15 July 2020; accepted 29 October 2020; published 10 November 2020)

Einstein-Podolsky-Rosen (EPR) steering has potential applications in quantum information processing. Here the genuine tripartite EPR steering is investigated in cascaded nonlinear process of spontaneous parametric down-conversion cascaded with a sum-frequency generation in an optical cavity for a wide range of the nonlinear parameters. The threshold properties of the cascaded nonlinear precess are also analyzed both below and without threshold regime, respectively. The genuine tripartite EPR steering is demonstrated based on the criteria for genuine multipartite EPR steering. Our scheme of the generation of genuine tripartite EPR steering can be used as a suggestion for the potential experiments and the applications in quantum communication and computation.

DOI: 10.1103/PhysRevA.102.052214

I. INTRODUCTION

Quantum nonlocality in quantum mechanics has received widespread attention in recent years. It is a large range, including quantum entanglement [1], quantum steering [2–4], quantum discord [5–7], and Bell nonlocality [8]. Quantum entanglement and Bell non-locality have been adequately investigated. In recent years, however, the issue of quantum steering which can be dated back to the famous Einstein-Podolsky-Rosen (EPR) paradox [9] has attracted a lot of interest. The essence of quantum steering was advanced by Schrödinger [2,3] in order to response the EPR paradox. Although this concept was proposed decades ago, scientists did not understand the true meaning of quantum steering. Until 2007, Wiseman *et al.* [10] gave the rigorous definition of quantum steering in the form of a task. Quantum steering (EPR steering) shows an unique asymmetry that is different from quantum entanglement and Bell nonlocality. It is precisely because of this characteristic of asymmetry that EPR steering has potential application prospects in many aspects such as quantum key distribution [11,12], quantum secret sharing [13–17], quantum networks [18], and so on.

A lot of studies have been done on the topic of EPR steering. The earliest demonstration of EPR steering was done in a nondegenerate optical parametric oscillator [19]. In a seminal work, an overview of achievements on EPR steering was shown by Reid *et al.* [20]. Continuous variable (CV) EPR steering was also investigated both in theory and in experiment [21–29] because CV can be unconditionally implemented. CV EPR steering can be detected by the criterion which proposed by Reid [30]. He and Reid [25] developed the concept of genuine N-partite EPR steering and put forward the criteria for multipartite EPR steering. Rosales-Zárate *et al.* [31] investigated the asymmetry of the decoherence effects on the EPR steering and they found that the direction of EPR steering is of great significance for understanding the decoherence of EPR steering. In 2017, Olsen [32] showed that one can control the asymmetry of EPR steering in the system by adjusting the amplitude of an injected signal. Bipartite asymmetry EPR steering was also investigated in the cascaded fourth-harmonic generation process [33] and the cascaded third-harmonic generation process [34], respectively. Tischler *et al.* [35] gave an experimental demonstration of one-way steering by using a sufficient condition for nonsteerability. Huang *et al.* [36] demonstrated that one can generate and control the asymmetry of steady-state EPR steering by engineering asymmetric couplings to the optical field in 2019. EPR steering was also investigated based on the cascaded four-wave mixing processes [37,38] and cascaded nonlinear processes in optical superlattice [39,40]. In addition, a necessary and sufficient characterization of steering was proposed based on a quantum information processing task [41]. Recently, Fadel *et al.* [42] presented criteria to detect entanglement and EPR steering between two bosonic modes through the measurements of number and phase. Xiang *et al.* [43] proposed symmetric and asymmetric structures of cascaded four-wave mixing to produce quadripartite EPR steering and investigated four distinct types of monogamy relations of Gaussian steering. In a word, EPR steering has received much attention, which made it become a useful quantum resource for quantum information.

The generation of tripartite entanglement was investigated through a spontaneous parametric down-conversion cascaded with a sum-frequency process both in an optical cavity [44–46] and without optical cavity [47] and the feasibility of the schemes were also theoretically demonstrated. However, up to now, the genuine multipartite EPR quantum steering correlations in this cascaded nonlinear process have not been studied. In this paper, we present the genuine tripartite EPR steering in the cascaded nonlinear processes of spontaneous parametric down-conversion cascaded with a sum-frequency generation in an optical cavity based on the criterion for multipartite EPR steering [25]. The quantum steering properties are discussed for a wide range of nonlinear

*ybyu@163.com
†aixichen@163.com

 ©2020 American Physical Society

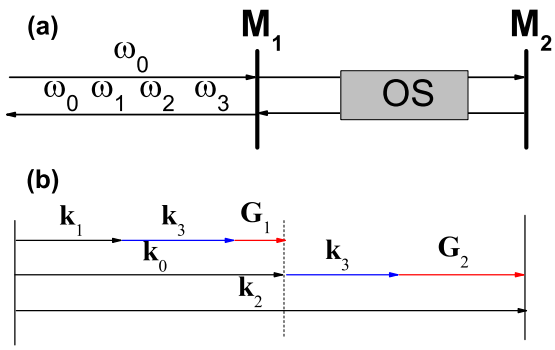

FIG. 1. (a) Sketch of the one-sided optical cavity in which an optical superlattice (OS) is placed as a nonlinear gain medium. (b) The quasi-phase-matching sketch for the cascaded nonlinear process as $\mathbf{k}_0 = \mathbf{k}_1 + \mathbf{k}_3 + \mathbf{G}_1$ and $\mathbf{k}_2 = \mathbf{k}_0 + \mathbf{k}_3 + \mathbf{G}_2$, where reciprocal vectors $\mathbf{G}_1$ and $\mathbf{G}_2$ are provided by OS.

parameters related to the cascaded nonlinear processes. The threshold properties of the system are also analyzed both below and without threshold, respectively. And we finally demonstrate the success of tripartite EPR steering in the cascaded nonlinear processes and discuss the experimental feasibility. The remaining part of this paper is organized as following. In Sec. II, we describe the Hamiltonian and the equations of motion obtained in the positive-P representation [48,49]. And we also performed fluctuation analysis and obtained stationary solutions. Detection of the genuine tripartite EPR steering is discussed in Sec. III. Through calculation and graph analysis, we show the effects of Fourier analysis frequency ω, nonlinear coupling parameter κ, pump value ϵ, and damping rates of γ on the tripartite EPR steering, respectively. Finally, a brief summary about this work is given in Sec. IV.

II. EQUATIONS OF MOTION AND THE STATIONARY SOLUTIONS

A. Equations of motion for the optical modes

We consider a pump with frequency of ω_0 incident into a one-sided optical cavity in which an optical superlattice (OS) is placed as a nonlinear gain medium, which can be seen in Fig. 1(a). Mirror M2 reflects all beams completely, while mirror M1 reflects all beams partially. First, two beams with the frequencies of ω_1 and ω_3 are generated by the first nonlinear process of spontaneous parametric down-conversion. Then, the third beam with frequency of ω_2 is generated by a cascaded sum-frequency generation process between pump and the beam with frequency of ω_3 in the same optical superlattice. The energy conservations in the cascaded nonlinear process are $\omega_0 = \omega_1 + \omega_3$ and $\omega_2 = \omega_0 + \omega_3$. This cascaded nonlinear process can be achieved by the technique of quasi-phase-matching [50], which can be seen in the similar experiment work [51,52]. The phase mismatch in the cascaded nonlinear process can be compensated by two reciprocal vectors $\mathbf{G}_1$ and $\mathbf{G}_2$ which provided by optical superlattice for $\mathbf{k}_0 = \mathbf{k}_1 + \mathbf{k}_3 + \mathbf{G}_1$ and $\mathbf{k}_2 = \mathbf{k}_0 + \mathbf{k}_3 + \mathbf{G}_2$, which can be seen in Fig. 1(b).

In order to derive the equations of motion and the stationary solutions, we start from the interaction Hamiltonian of this cascaded nonlinear process as

$$\mathcal{H}_I = i\hbar\kappa_1\hat{b}\hat{a}_1^\dagger\hat{a}_3^\dagger + i\hbar\kappa_2\hat{b}\hat{a}_3\hat{a}_2^\dagger + \text{H.c.}, \tag{1}$$

where κ_1 and κ_2 represent the dimensionless effective nonlinearity that are related to pump power, nonlinear polarizability, and the structure parameters of the optical superlattice. They are taken to be real for the purpose of simplicity [53]. $\hat{b}$ and $\hat{a}_i$ $(i = 1, 2, 3)$ are the bosonic annihilation operator of the cavity modes with frequency of ω_i (i=0,1,2,3), respectively. The Hamiltonian of the coherent input cavity pumping can be written as [49]

$$\mathcal{H}_{\text{pump}} = i\hbar(\epsilon\hat{b}^\dagger - \epsilon^*\hat{b}), \tag{2}$$

where ϵ represents the coherent optical field with the frequency of ω_0 incident on the optical cavity. Following the description of Lindblad superoperator [49], the damping of the four optical fields into a zero temperature Markovian reservoir can be described by the Lindblad superoperator

$$\begin{aligned}\mathcal{L}\hat{\rho} = {} & \gamma_0(2\hat{b}\hat{\rho}\hat{b}^\dagger - \hat{b}^\dagger\hat{b}\hat{\rho} - \hat{\rho}\hat{b}^\dagger\hat{b}) \\ & + \gamma_i(2\hat{a}_i\hat{\rho}\hat{a}_i^\dagger - \hat{a}_i^\dagger\hat{a}_i\hat{\rho} - \hat{\rho}\hat{a}_i^\dagger\hat{a}_i),\end{aligned} \tag{3}$$

where $\hat{\rho}$ is the system density matrix and $\gamma_i (i = 0, 1, 2, 3)$ represents the cavity loss at ω_i, respectively. The damping rates γ_i is related to the reflection transmission coefficient of the optical cavity for $r_i = 1 - \gamma_i$ and $t_i = \sqrt{2\gamma_i}$ [44]. The master equation of this system can be expressed as

$$\frac{d\hat{\rho}}{dt} = -\frac{i}{\hbar}[\mathcal{H}_I + \mathcal{H}_{\text{pump}}, \hat{\rho}] + \sum \mathcal{L}\hat{\rho}. \tag{4}$$

One can map the master equation onto Fokker-Planck equation (FPE) in pseudoprobability distribution [49]. However, one cannot obtain stochastic differential equations from FPE because the FPE for the Glauber-Sudarshan P function [54,55] has a negative diffusion matrix. Positive-P representation [48,49] is exact for this cascaded system and can be used in our discussion. The FPE can be found from the equation of the Glauber-Sudarshan P distribution by taking variables and their complex conjugates as independent [56]. Therefore, α_i and α_i^+ are independent variables in the following, which correspond to α_i and $\alpha_i^\dagger$ when the averages of products converge to normally ordered operator expectation values [56] and similarly for β. In addition, in positive-P representation, $P(\alpha_i, \beta)$ function always exists for a physical density operator and has all the properties of a genuine probability [49]. Then, we obtained the FPE of the system, which has a positive-definite diffusion matrix as

$$\begin{aligned}\frac{dP(\alpha_i,\beta)}{dt} = \Bigg\{-\Bigg[& (-\gamma_1\alpha_1 + \kappa_1\alpha_3^+\beta)\frac{\partial}{\partial\alpha_1} + (-\gamma_1\alpha_1^+ + \kappa_1\alpha_3\beta^+)\frac{\partial}{\partial\alpha_1^+} + (-\gamma_2\alpha_2 + \kappa_2\alpha_3\beta)\frac{\partial}{\partial\alpha_2} \\ & + (-\gamma_2\alpha_2^+ + \kappa_2\alpha_3^+\beta^+)\frac{\partial}{\partial\alpha_2^+} + (-\gamma_3\alpha_3 + \kappa_1\alpha_1^+\beta - \kappa_2\alpha_2\beta^+)\frac{\partial}{\partial\alpha_3}\end{aligned}$$

$$
\begin{aligned}
&+(-\gamma_3\alpha_3^+ + \kappa_1\alpha_1\beta^+ - \kappa_2\alpha_2^+\beta)\frac{\partial}{\partial\alpha_3^+} + \frac{\partial}{\partial\beta}(-\gamma_0\beta + \epsilon - \kappa_1\alpha_1\alpha_3 - \kappa_2\alpha_2\alpha_3^+) \\
&+ \frac{\partial}{\partial\beta^*}(-\gamma_0\beta^+ + \epsilon^* - \kappa_1\alpha_1^+\alpha_3^+ - \kappa_2\alpha_2^+\alpha_3)\Bigg] \\
&+ \frac{1}{2}\left(\frac{\partial^2}{\partial\alpha_1\partial\alpha_3}2\kappa_1\beta\right) + \frac{1}{2}\left(\frac{\partial^2}{\partial\alpha_1^+\partial\alpha_3^+}2\kappa_1\beta^+\right) \\
&- \frac{1}{2}\left(\frac{\partial^2}{\partial\alpha_3\partial\beta}2\kappa_2\alpha_2^+\right) - \frac{1}{2}\left(\frac{\partial^2}{\partial\alpha_3^+\partial\beta^+}2\kappa_2\alpha_2\right)\Bigg\}P(\alpha_i,\beta).
\end{aligned} \tag{5}
$$

Following the normal processing [49], the equations of motion of the system can be derived in the positive-P representation [48,49],

$$
\begin{aligned}
\frac{d\alpha_1}{dt} &= -\gamma_1\alpha_1 + \kappa_1\alpha_3^+\beta + \sqrt{\kappa_1\beta/2}(\eta_1 + i\eta_2), \quad \frac{d\alpha_1^+}{dt} = -\gamma_1\alpha_1 + \kappa_1\alpha_3\beta^+ + \sqrt{\kappa_1\beta^+/2}(\eta_3 + i\eta_4), \\
\frac{d\alpha_2}{dt} &= -\gamma_2\alpha_2 + \kappa_2\alpha_3\beta, \quad \frac{d\alpha_2^+}{dt} = -\gamma_2\alpha_2^+ + \kappa_2\alpha_3^+\beta^+, \\
\frac{d\alpha_3}{dt} &= -\gamma_3\alpha_3 + \kappa_1\alpha_1^+\beta - \kappa_2\alpha_2\beta^+ + \sqrt{\kappa_1\beta/2}(\eta_1 - i\eta_2) + \sqrt{-\kappa_2\alpha_2^+/2}(\eta_5 + i\eta_6), \\
\frac{d\alpha_3^+}{dt} &= -\gamma_3\alpha_3^+ + \kappa_1\alpha_1\beta^+ - \kappa_2\alpha_2^+\beta + \sqrt{\kappa_1\beta^+/2}(\eta_3 - i\eta_4) + \sqrt{-\kappa_2\alpha_2/2}(\eta_7 + i\eta_8), \\
\frac{d\beta}{dt} &= \epsilon - \gamma_0\beta - \kappa_1\alpha_1\alpha_3 - \kappa_2\alpha_2\alpha_3^+ + \sqrt{-\kappa_2\alpha_2^+/2}(\eta_5 - i\eta_6), \\
\frac{d\beta^+}{dt} &= \epsilon^* - \gamma_0\beta^+ - \kappa_1\alpha_1^+\alpha_3^+ - \kappa_2\alpha_2^+\alpha_3 + \sqrt{-\kappa_2\alpha_2/2}(\eta_7 - i\eta_8),
\end{aligned} \tag{6}
$$

where $\eta_i(t)$ are the Gaussian noise terms with the properties $\langle\eta_i(t)\rangle = 0$ and $\langle\eta_i(t)\eta_j(t')\rangle = \delta_{ij}\delta(t-t')$.

B. Steady-state solutions

Equation (6) cannot to be solved analytically. However, we can decompose the positive-P variables [49] into their steady-state expectation values and a small part of Gaussian fluctuations as $\alpha_i = A_i + \delta\alpha_i$ $(i = 1, 2, 3)$ and similarly for β, where $A_i = \langle\alpha_i\rangle$ is the steady-state solution for the optical mode with the frequency of ω_i. Based on above calculations, by means of linear processing approach [49], Eq. (6) can be rewritten for the fluctuation terms as

$$
d\delta\tilde{\alpha} = -\mathbf{A}\delta\tilde{\alpha}dt + \mathbf{B}dW, \tag{7}
$$

with

$$
\delta\tilde{\alpha} = [\delta\alpha_1, \delta\alpha_1^\dagger, \delta\alpha_2, \delta\alpha_2^\dagger, \delta\alpha_3, \delta\alpha_3^\dagger, \delta\beta, \delta\beta^\dagger]^{\mathrm{T}}, \tag{8}
$$

where $\mathbf{A}$ is the drift matrix, $\mathbf{B}$ contains the steady-state solutions of noise terms and dW is a vector of Wiener increments [49]. The drift matrix $\mathbf{A}$ can be written as

$$
\mathbf{A} = \begin{pmatrix}
\gamma_1 & 0 & 0 & 0 & 0 & -\kappa_1 A_0 & \kappa_1 A_3^* & 0 \\
0 & \gamma_1 & 0 & 0 & -\kappa_1 A_0^* & 0 & 0 & -\kappa_1 A_3 \\
0 & 0 & \gamma_2 & 0 & -\kappa_2 A_0 & 0 & -\kappa_2 A_3 & 0 \\
0 & 0 & 0 & \gamma_2 & 0 & -\kappa_2 A_0^* & 0 & -\kappa_2 A_3^* \\
0 & -\kappa_1 A_0 & \kappa_2 A_0^* & 0 & \gamma_3 & 0 & -\kappa_1 A_1^* & \kappa_2 A_2 \\
-\kappa_1 A_0^* & 0 & 0 & \kappa_2 A_0 & 0 & \gamma_3 & \kappa_2 A_2^* & -\kappa_1 A_1 \\
\kappa_1 A_3 & 0 & \kappa_2 A_3^* & 0 & \kappa_1 A_1 & \kappa_2 A_2 & \gamma_0 & 0 \\
0 & \kappa_1 A_3^* & 0 & \kappa_2 A_3 & \kappa_2 A_2^* & \kappa_1 A_1^* & 0 & \gamma_0
\end{pmatrix}. \tag{9}
$$

Through the above discussion, the drift matrix $\mathbf{A}$ should be a positive-definite matrix which requires there are no negative real part eigenvalues for $\mathbf{A}$. In this case, the system can be in a steady-state and above linearization process is effective. Eq. (7) can be solved by Fourier transform [49]. Then, the satisfaction of the condition of matrix $\mathbf{A}$ allows us to calculate the intracavity spectra via the intracavity spectral matrix [49]

$$
\mathbf{S}(\omega) = (\mathbf{A} + i\omega\mathbf{I})^{-1}\mathbf{D}(\mathbf{A}^{\mathrm{T}} - i\omega\mathbf{I})^{-1}, \tag{10}
$$

where ω is the Fourier analysis frequency, $\mathbf{I}$ is the identity matrix, and $\mathbf{D} = \mathbf{B}\mathbf{B}^{\mathrm{T}}$. According to the standard input-output

relationship [57], we can obtain the output spectrum of the cavity.

From Eq. (6), throwing away the noise terms, one can obtain the mean values for the equations of motion as

$$\begin{aligned}\frac{d\langle\alpha_1\rangle}{dt} &= -\gamma_1\langle\alpha_1\rangle + \kappa_1\langle\alpha_3^*\rangle\langle\beta\rangle,\\ \frac{d\langle\alpha_2\rangle}{dt} &= -\gamma_2\langle\alpha_2\rangle + \kappa_2\langle\alpha_3\rangle\langle\beta\rangle,\\ \frac{d\langle\alpha_3\rangle}{dt} &= -\gamma_3\langle\alpha_3\rangle + \kappa_1\langle\alpha_1^*\rangle\langle\beta\rangle - \kappa_2\langle\alpha_2\rangle\langle\beta^*\rangle,\\ \frac{d\langle\beta\rangle}{dt} &= \epsilon - \gamma_0\langle\beta\rangle - \kappa_1\langle\alpha_1\rangle\langle\alpha_3\rangle - \kappa_2\langle\alpha_2\rangle\langle\alpha_3^*\rangle. \quad (11)\end{aligned}$$

The steady-state solutions A_i can be obtained by setting $\frac{d\langle\alpha_i\rangle}{dt} = 0$ and $\frac{d\langle\beta\rangle}{dt} = 0$ in Eq. (11). We find that the steady-state solutions obtained from Eq. (11) are divided into three different categories and it is determined by whether there is a oscillation threshold. If $\kappa_1^2\gamma_2 > \kappa_2^2\gamma_1$, the system has a threshold

$$\epsilon_c = \frac{\gamma_0\sqrt{\gamma_1\gamma_2\gamma_3}}{\sqrt{\kappa_1^2\gamma_2 - \kappa_2^2\gamma_1}}. \quad (12)$$

1. Below the threshold

The cavity will not oscillate below this threshold and the signal modes will not be macroscopically occupied when the value of ϵ below the threshold ϵ_c. We obtain the steady-state solutions in this case ($\epsilon < \epsilon_c$) as

$$A_0 = \frac{\epsilon}{\gamma_0}, \quad A_i = 0\ (i = 1, 2, 3). \quad (13)$$

2. Above the threshold

In the second case of $\epsilon > \epsilon_c$, we obtain the steady-state solutions from Eq. (11) as

$$\begin{aligned}&A_0 = \frac{\epsilon_c}{\gamma_0}, \quad A_1 = \frac{\kappa_1}{\gamma_1}A_0A_3, \quad A_2 = \frac{\kappa_2}{\gamma_2}A_0A_3,\\ &A_3 = \sqrt{\frac{\epsilon - \epsilon_c}{\frac{\epsilon_c}{\gamma_0}\left(\frac{\kappa_1^2}{\gamma_1} + \frac{\kappa_2^2}{\gamma_2}\right)}}. \quad (14)\end{aligned}$$

3. Without threshold

We find that there is no threshold if $\kappa_1^2\gamma_2 < \kappa_2^2\gamma_1$, which means that for any value of the pumping field, the signal modes will not be occupied macroscopically. In this case, the steady-state solutions are obtained as

$$A_0 = \frac{\epsilon}{\gamma_0}, \quad A_i\ (i = 1, 2, 3) = 0, \quad (15)$$

which is the same as the case below the threshold. If there is no sum-frequency process and only down-conversion process, then $\kappa_2 = 0$ and $\gamma_2 = 1$, the threshold in Eq. (12) will become the threshold of nondegenerate optical parametric oscillation (NOPO) as $\epsilon_0 = \frac{\gamma_0\sqrt{\gamma_1\gamma_3}}{\kappa_1}$. If it is a degenerate OPO, $\gamma_1 = \gamma_3 = \gamma$, the threshold is the normal OPO threshold $\epsilon_{th} = \frac{\gamma_0\gamma}{\kappa_1}$ [56]. In order to facilitate the discussion for without threshold, in the later calculation, we will express the pump field ϵ in a ratio of ϵ_0 in the range of without threshold.

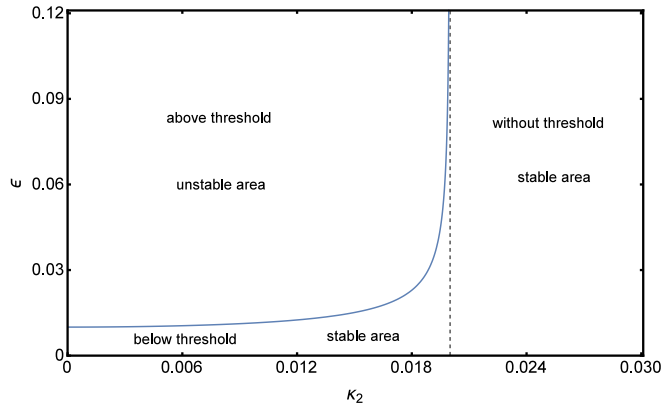

FIG. 2. The steady-state range with $\gamma_0 = 0.01$, $\gamma_1 = \gamma_2 = \gamma_3 = 0.02$, and $\kappa_1 = 0.02$. The dashed line is the separated line with and without threshold.

C. Steady-state analysis

We have already obtained the steady-state values in different situations. However, the drift matrix **A** should be a positive-definite matrix which requires that the eigenvalue of **A** must not have a negative real part. In the following, we will proceed to the steady-state analysis starting from analyzing the eigenvalues of the drift matrix **A** in Eq. (9) to verify the effectiveness of the linearization process. The polynomial of eigenvalues for matrix **A** can be obtained as

$$\begin{aligned}(\gamma_0 - J)^2\big[(\gamma_1 - J)(\gamma_2 - J)(\gamma_3 - J) + JA_0^2\big(\kappa_1^2 - \kappa_2^2\big)\\ + A_0^2\big(\kappa_2^2\gamma_1 - \kappa_1^2\gamma_2\big)\big]^2 = 0, \quad (16)\end{aligned}$$

where J is the required eigenvalue, which should have eight values. In order to simplify the calculation, we set $\gamma_1 = \gamma_2 = \gamma_3 = \gamma$. The damping rates γ_i is related to the reflection transmission coefficient of the optical cavity for $r_i = 1 - \gamma_i$ and $t_i = \sqrt{2\gamma_i}$ [44]. So experimentally, one can design the same reflection and transmittance to get the same damping rate for the three beams. In this case, the threshold of Eq. (12) can be rewritten as $\epsilon_c = \frac{\gamma\gamma_0}{\sqrt{\kappa_1^2-\kappa_2^2}}$. Then, we obtain the expression of the eigenvalues as

$$\begin{aligned}&J_{1,2} = \gamma_0, \quad J_{3,4} = \gamma, \quad J_{5,6} = \gamma + \frac{\epsilon}{\gamma_0}\sqrt{\kappa_1^2 - \kappa_2^2},\\ &J_{7,8} = \gamma - \frac{\epsilon}{\gamma_0}\sqrt{\kappa_1^2 - \kappa_2^2}. \quad (17)\end{aligned}$$

We find that the last two eigenvalues $J_{7,8}$ in Eq. (17) may have a negative real part when $\epsilon > \frac{\gamma\gamma_0}{\sqrt{\kappa_1^2-\kappa_2^2}}$, which means that linearization is invalid for the case above the threshold. That is to say, the fluctuations above the threshold cannot be linearized because the solution is unstable and there is no steady-state solutions to linearize around. In the ranges below the threshold and without threshold, one can find that none of the eigenvalues in Eq. (17) have negative real part, which indicates that the system is always stable in the ranges below the threshold and without threshold.

In Fig. 2 we plot the steady-state range with $\gamma_0 = 0.01$, $\gamma_1 = \gamma_2 = \gamma_3 = 0.02$, and $\kappa_1 = 0.02$. The dashed line is the separated line for with and without threshold. The system is

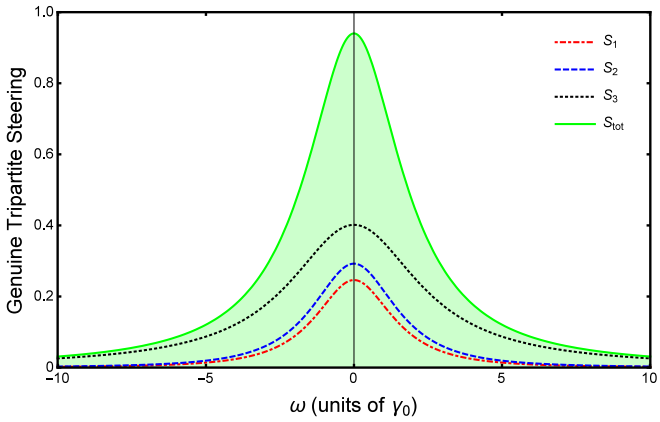

FIG. 3. The values of S_i and $S_{\rm tot}$ below threshold versus the Fourier analysis frequency ω with $\gamma_0 = 0.01$, $\gamma_1 = \gamma_2 = \gamma_3 = 0.02$, $\kappa_1 = 0.02$, $\kappa_2 = 0.5\kappa_1$, and $\epsilon = 0.3\epsilon_c$.

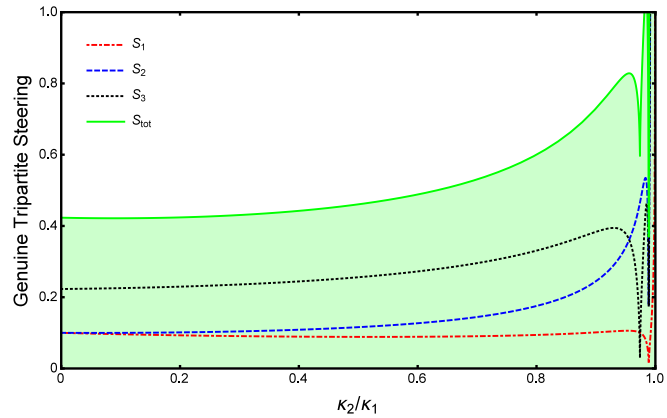

FIG. 5. The values of S_i and $S_{\rm tot}$ below threshold versus the nonlinear coupling parameter κ_2/κ_1 with $\gamma_0 = 0.01$, $\gamma_1 = \gamma_2 = \gamma_3 = 0.02$, $\kappa_1 = 0.02$, $\epsilon = 0.3\epsilon_c$, and $\omega = 2\gamma_0$.

always unstable above the solid line. The system is stable in the ranges of below the solid line (below the threshold range) and the right of the dashed line (without threshold range). Therefore, we can perform linearized fluctuation analysis and discuss the EPR steering properties in above two stable ranges in the following.

III. GENUINE TRIPARTITE EPR STEERING

Bipartite asymmetric quantum steering was investigated in NOPO with an injected signal [32], cascaded fourth-harmonic generation [33], and third-harmonic generation [34], respectively. Genuine tripartite quantum steering among pump, second-harmonic, and third-harmonic was demonstrated theoretically in our previous work [39]. And the genuine tripartite quantum steering in cascaded nonlinear process of quasi-phase-matching fourth-harmonic generation in an optical cavity was also confirmed [40]. In this paper, the genuine tripartite EPR steering in nonlinear processes of spontaneous parametric down-conversion cascaded a sum-frequency generation in an optical cavity is investigated according to the criteria of multipartite EPR steering [25]. The orthogonal quadrature is defined as $\alpha_i = X_i + iY_i$, and $\alpha_i^\dagger = X_i - iY_i$, where X_i and Y_i represents quadrature amplitude and phase component, respectively. Based on the criteria of multipartite EPR steering [25], one can use a set of conditions to investigate whether does EPR steering exist in the system. And a set of inequalities is given as

$$\begin{aligned} S_1 &= \Delta(X_1 - X_2)\Delta(Y_1 + Y_2 + Y_3) < 1, \\ S_2 &= \Delta(X_2 - X_3)\Delta(Y_1 + Y_2 + Y_3) < 1, \\ S_3 &= \Delta(X_3 - X_1)\Delta(Y_1 + Y_2 + Y_3) < 1. \end{aligned} \tag{18}$$

When the values of $S_i < 1 (i = 1, 2, 3)$, EPR steering of system i will be confirmed [25]. That is the steering of 1 will be confirmed by the other optical fields $\{2, 3\}$ if $S_1 < 1$, steering of 2 will be confirmed by the other optical fields $\{3, 1\}$ if $S_2 < 1$, and steering of 3 will be confirmed by the other optical fields $\{1, 2\}$ if $S_3 < 1$. And it also indicates that the three fields are bipartite quantum steering with each other. The most important condition for verifying tripartite EPR steering

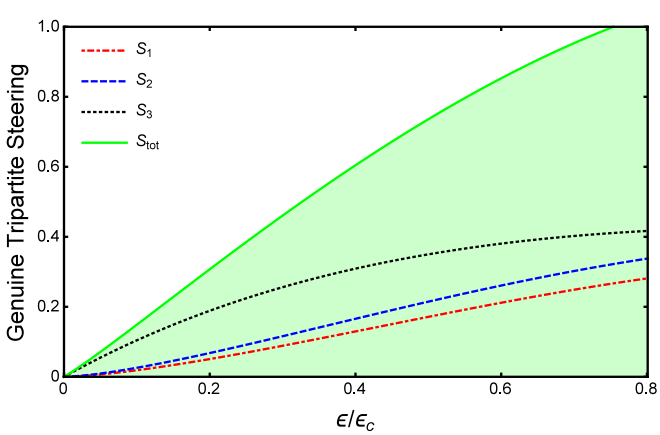

FIG. 4. The values of S_i and $S_{\rm tot}$ below threshold versus the varied pump value ϵ with $\gamma_0 = 0.01$, $\gamma_1 = \gamma_2 = \gamma_3 = 0.02$, $\kappa_1 = 0.02$, $\kappa_2 = 0.5\kappa_1$, and $\omega = 2\gamma_0$.

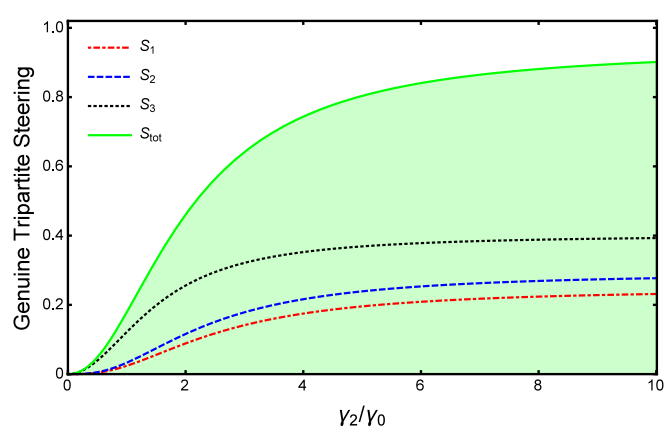

FIG. 6. The values of S_i and $S_{\rm tot}$ below threshold versus the damping rates of γ/γ_0 with $\gamma_0 = 0.01$, $\kappa_1 = 0.02$, $\kappa_2 = 0.5\kappa_1$, $\omega = 2\gamma_0$, and $\epsilon = 0.3\epsilon_c$.

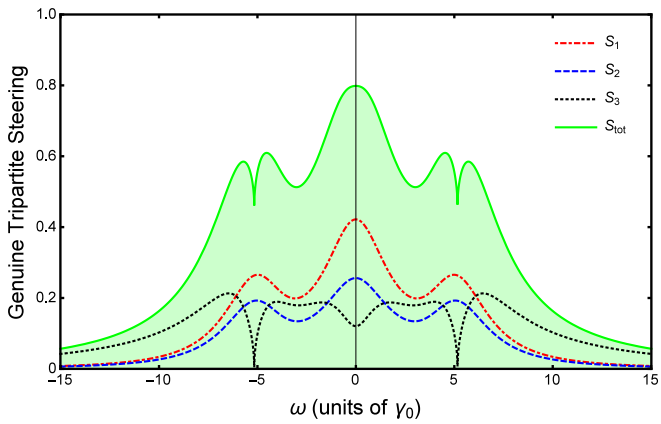

FIG. 7. The values of S_i and S_{tot} without threshold versus the Fourier analysis frequency ω with $\gamma_0 = 0.01$, $\gamma_1 = \gamma_2 = \gamma_3 = 0.02$, $\kappa_1 = 0.02$, $\kappa_2 = 2.5\kappa_1$, and $\epsilon = 1.1\epsilon_0$.

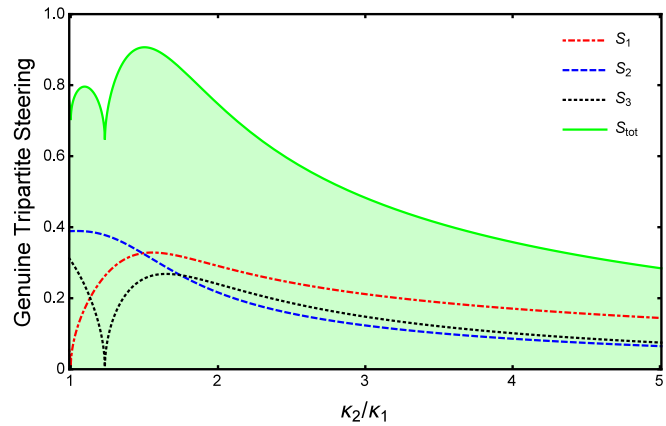

FIG. 9. The values of S_i and S_{tot} without threshold versus the nonlinear coupling parameter κ_2/κ_1 with $\gamma_0 = 0.01$, $\gamma_1 = \gamma_2 = \gamma_3 = 0.02$, $\kappa_1 = 0.02$, $\epsilon = 1.1\epsilon_0$, and $\omega = 2\gamma_0$.

is the measurement of

$$S_{tot} = S_1 + S_2 + S_3 < 1. \tag{19}$$

Satisfying Eq. (19) will demonstrate that tripartite EPR steering exists in the system [25]. The parameters will greatly influence the calculation results. In the following, we will investigate the EPR steering in the two ranges of below the threshold and without threshold.

A. Tripartite EPR steering in the range of below the threshold

Figure 3 depicts that S_i and S_{tot} versus the Fourier analysis frequency ω with $\gamma_0 = 0.01$, $\gamma_1 = \gamma_2 = \gamma_3 = 0.02$, $\kappa_1 = 0.02$, and $\kappa_2 = 0.5\kappa_1$. One can see clearly that the value of S_i are all below 1, and more importantly, S_{tot} is also below 1 in the whole range of ω and Eq. (19) is satisfied. It shows that tripartite EPR steering can be generated by the cascaded nonlinear process. In Fig. 4, we show that the EPR steering varies with the pump value ϵ. Before the value of ϵ/ϵ_c reaches about 0.75, the value of S_{tot} increases as the threshold approaches, and is smaller than 1, which means that it is sufficient for the demonstration of tripartite EPR steering when $\epsilon < 0.75\epsilon_c$. However, S_{tot} violates the condition of tripartite EPR steering in Eq. (19) when the value of ϵ/ϵ_c is more than 0.75, which means that the tripartite EPR steering disappear in this case. Figure 5 shows that S_i and S_{tot} versus the nonlinear coupling parameter κ_2/κ_1 with $\gamma_1 = \gamma_2 = \gamma_3 = 0.02$ and $\omega = 2\gamma_0$. It can be seen clearly that S_{tot} is below 1 with the increase of κ_2/κ_1, which shows that tripartite EPR steering can be produced in our scheme. Nevertheless, the values of S_i and S_{tot} have mutated at about $\kappa_2/\kappa_1 = 1$, which because in the specific expressions of S_i and S_{tot}, the denominator is very small when the value of κ_2/κ_1 approaches 1 and the value of S_i and S_{tot} suddenly increases sharply and the threshold ϵ_c in Eq. (12) also becomes infinite. Actually, $\kappa_2/\kappa_1 < 1$ is the condition that the system has a threshold. We consider the influences of the damping rates of γ/γ_0 on the S_i and S_{tot}, which are plotted as a function of γ/γ_0 in Fig. 6. Obviously, S_{tot} satisfies the condition in Eq. (19). In other words, the genuine tripartite EPR steering can be generated by this cascaded nonlinear process in the range of below the threshold.

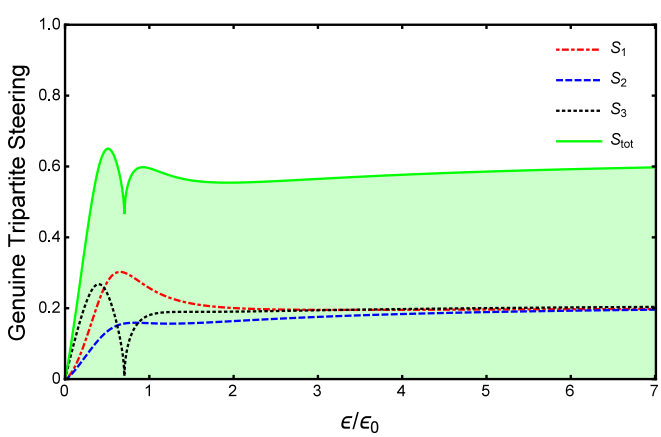

FIG. 8. The values of S_i and S_{tot} without threshold versus the varied pump value ϵ with $\gamma_0 = 0.01$, $\gamma_1 = \gamma_2 = \gamma_3 = 0.02$, $\kappa_1 = 0.02$, $\kappa_2 = 2.5\kappa_1$, and $\omega = 2\gamma_0$.

B. Tripartite EPR steering in the range of without threshold

In the range of without an oscillation threshold, linearized fluctuation analysis is also valid. We show that S_i and S_{tot} versus the Fourier analysis frequency ω in Fig. 7 with $\kappa_2 = 2.5\kappa_1$, $\epsilon = 1.1\epsilon_0$, and other parameters are consistent with the case in Fig. 3. The curves of S_i and S_{tot} are very symmetrical and the value of S_{tot} is below 1 in the whole range, which indicates that the genuine tripartite EPR steering can be produced in our scheme. In addition, there is a strong dip for S_3 at $\omega = 5$. It is because the optical fields of $\hat{a}_1$ and $\hat{a}_3$ are produced from the nonlinear process of spontaneous parametric down-conversion and they have a strong quantum correlation. Similar cases also can be seen in Figs. 8, 9, and 10. Then, we also investigate the effects of the pumping parameter ϵ and the effective nonlinear coupling parameter κ_2/κ_1 on the values of S_i and S_{tot} in Figs. 8 and 9, respectively. None of S_{tot} violates the condition of the tripartite EPR steering in Eq. (19) for the whole range of ϵ. Figure 9 shows that the

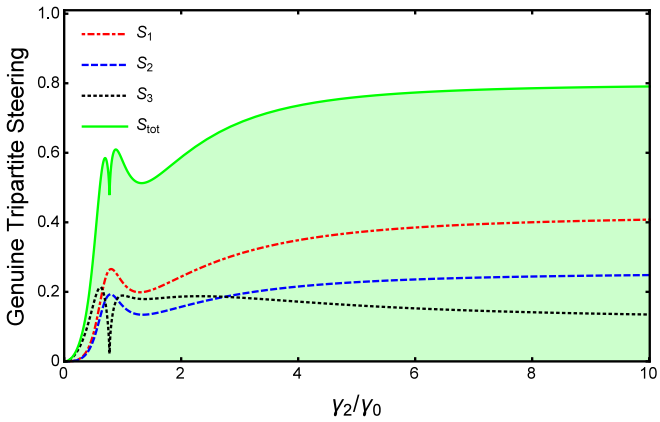

FIG. 10. The values of S_i and $S_{\rm tot}$ without threshold versus the damping rates of γ/γ_0 with $\kappa_1 = 0.02$, $\kappa_2 = 2.5\kappa_1$, $\omega = 2\gamma_0$, and $\epsilon = 1.1\epsilon_0$.

values of the S_i and $S_{\rm tot}$ are all below 1 and decrease with the increase of the effective nonlinear parameter κ_2/κ_1. We also show how the correlations of S_i and $S_{\rm tot}$ change as the damping rates of γ/γ_0 in Fig. 10. The value of $S_{\rm tot}$ is below 1, which demonstrates the success of the present scheme of the generation of genuine tripartite EPR steering again. In this way, the genuine tripartite EPR steering is demonstrated when the system has no threshold.

C. Discussions and experimental feasibility analysis

Through the above calculation, we find that various parameters have great influence on the tripartite EPR steering. The most crucial parameters are the damping rates γ_i and the effective nonlinear parameter κ_i. The damping rates γ_i is related to the reflection transmission coefficient of the optical cavity for $r_i = 1 - \gamma_i$ and $t_i = \sqrt{2\gamma_i}$ [44]. For example, in our calculation, we set $\gamma_1 = \gamma_2 = \gamma_3 = \gamma = 0.02$, that is, the transmittance of the coupling mirror M1 to the optical fields $\hat{a}_1, \hat{a}_2$ and $\hat{a}_3$ is $t_i^2 = 2\gamma = 4\%$ and the reflectivity is $r_i^2 = (1-\gamma)^2 = 96\%$. This can be achieved experimentally by coating the cavity mirror.

The nonlinear coupling parameter κ_i is related to pump power, nonlinear polarizability, and the structure parameters of optical superlattice. In our present scheme, we can change the nonlinear coupling parameter κ_i by designing the parameters of optical superlattice [51], which is the advantage of our scheme over the previous atomic system scheme in Refs. [37,38,43]. Moreover, the larger κ_2 can increase the conversion efficiency of the second cascaded nonlinear process, thus a better tripartite EPR steering can be obtained, which can be seen from Fig. 9. In this way, we can get a better tripartite EPR steering by designing optical superlattice and increasing the nonlinear coefficient κ_2. That is, it is more likely to get a better tripartite EPR steering in the range of without threshold than below the threshold.

In addition, the present scheme is more feasible in experiment than our previous schemes in Refs. [39,40] because both the single pass process [51] of this cascaded nonlinear process and the OPO scheme [52] have been realized experimentally. In the single pass process [51], 666-nm signal and 2644-nm idler were generated by the first parametric down-conversion process. Then 443-nm sum-frequency beam was generated by the sum-frequency process between 532-nm pump and 2644-nm idler. The maximum conversion efficiency of the 666 nm signal is up to 34.0% and the 443 nm sum-frequency beam is about 3%. In the OPO scheme [52], 633-nm signal and 3342-nm idler were generated by the first nonlinear process of parametric down-conversion. A 459-nm sum-frequency beam was generated by the cascaded sum-frequency process between 532-nm pump and 3342-nm idler. However, in their OPO scheme, only 633-nm signal resonates, and other beams do not resonate in the cavity. It is difficult to make all the beams resonate in the cavity at the same time, which is also the biggest challenge of our present scheme in this paper. Based on the experiment of the generation of three-color entanglement [58], we think that through careful design and control, it should be possible to realize the simultaneous resonance of three beams in the cavity.

IV. CONCLUSIONS

In this paper, we investigate the genuine tripartite EPR steering in the cascaded nonlinear process of spontaneous parametric down-conversion coupled with a sum-frequency generation in an optical cavity for a wide range of the parameters. The threshold properties of the system are also analyzed. We found that the genuine tripartite EPR steering can be achieved in the ranges below the threshold and without threshold based on the criteria for genuine multipartite EPR steering which proposed by He and Reid [25]. The influences of nonlinear coupling parameter κ and the damping rates of γ/γ_0 on the tripartite EPR steering are investigated. The nonlinear coupling parameter κ_i is related to pump power, nonlinear polarizability, and the structure parameters of optical superlattice. The damping rates γ_i are related to the reflection transmission coefficient of the optical cavity. Therefore, one can obtain better tripartite EPR steering by designing optical superlattice structure and choosing the appropriate reflection transmission coefficient. However, the demonstration of genuine tripartite EPR steering above the threshold has not been successful in the present study because the linearization process is ineffective in the range of above the threshold. Maybe one can employ other methods to prove the tripartite even quadripartite (including pump) EPR steering above the threshold by avoiding linearization of the fluctuation. We think that our scheme can be used as a suggestion for potential experiments and the potential applications in quantum information processing.

ACKNOWLEDGMENTS

This work is supported by National Natural Science Foundations of China (No. 61975184 and No. 12075209), Zhejiang Provincial Natural Science Foundation of China (No. LY18A040007), Science Foundation of Zhejiang Sci-Tech University (No. 19062151-Y and No. 18062145-Y) and Open Foundation of Key Laboratory of Optical Field Manipulation of Zhejiang Province (No. ZJOFM-2019-002).

[1] R. Horodecki, P. Horodecki, M. Horodecki, and K. Horodecki, Quantum entanglement, Rev. Mod. Phys. **81**, 865 (2009).
[2] E. Schrödinger, Discussion of probability relations between separated systems, Math. Proc. Cambridge Philos. Soc. **32**, 446 (1936).
[3] E. Schrödinger, Discussion of probability relations between separated systems, Math. Proc. Cambridge Philos. Soc. **31**, 555 (1935).
[4] R. Uola, A. C. S. Costa, H. C. Nguyen, and O. Gühne, Quantum steering, Rev. Mod. Phys. **92**, 015001 (2020).
[5] H. Ollivier and W. H. Zurek, Quantum Discord: A Measure of the Quantumness of Correlations, Phys. Rev. Lett. **88**, 017901 (2001).
[6] A. Datta, A. Shaji, and C. M. Caves, Quantum Discord and the Power of One Qubit, Phys. Rev. Lett. **100**, 050502 (2008).
[7] K. Modi, A. Brodutch, H. Cable, T. Paterek, and V. Vedral, The classical-quantum boundary for correlations: Discord and related measures, Rev. Mod. Phys. **84**, 1655 (2012).
[8] J. S. Bell, On the Einstein Podolsky Rosen paradox, Physics **1**, 195 (1964).
[9] A. Einstein, B. Podolsky, and N. Rosen, Can quantum-mechanical description of physical reality be considered complete? Phys. Rev. **47**, 777 (1935).
[10] H. M. Wiseman, S. J. Jones, and A. C. Doherty, Steering, Entanglement, Nonlocality, and the Einstein-Podolsky-Rosen Paradox, Phys. Rev. Lett. **98**, 140402 (2007).
[11] N. Walk, S. Hosseini, J. Geng, O. Thearle, J. Y. Haw, S. Armstrong, S. M. Assad, J. Janousek, T. C. Ralph, T. Symul, H. M. Wiseman, and P. K. Lam, Experimental demonstration of Gaussian protocols for one-sided device-independent quantum key distribution, Optica **3**, 634 (2016).
[12] C. Branciard, E. G. Cavalcanti, S. P. Walborn, V. Scarani, and H. M. Wiseman, One-sided device-independent quantum key distribution: Security, feasibility, and the connection with steering, Phys. Rev. A **85**, 010301(R) (2012).
[13] M. Hillery, V. Bužek, and A. Berthiaume, Quantum secret sharing, Phys. Rev. A **59**, 1829 (1999).
[14] S. Gaertner, C. Kurtsiefer, M. Bourennane, and H. Weinfurter, Experimental Demonstration of Four-Party Quantum Secret Sharing, Phys. Rev. Lett. **98**, 020503 (2007).
[15] A. M. Lance, T. Symul, W. P. Bowen, T. Tyc, B. C. Sanders, and P. K. Lam, Continuous variable (2, 3) threshold quantum secret sharing schemes, New J. Phys. **5**, 4 (2003).
[16] Y. A. Chen, A. N. Zhang, Z. Zhao, X. Q. Zhou, C. Y. Lu, C. Z. Peng, T. Yang, and J. W. Pan, Experimental Quantum Secret Sharing and Third-Man Quantum Cryptography, Phys. Rev. Lett. **95**, 200502 (2005).
[17] Y. Xiang, I. Kogias, G. Adesso, and Q. Y. He, Multipartite Gaussian steering: Monogamy constraints and quantum cryptography application, Phys. Rev. A **95**, 010101(R) (2017).
[18] D. Cavalcanti, P. Skrzypczyk, G. H. Aguilar, R. V. Nery, P. H. S. Ribeiro, and S. P. Walborn, Detection of entanglement in asymmetric quantum networks and multipartite quantum steering, Nat. Commun. **6**, 7941 (2015).
[19] Z. Y. Ou, S. F. Pereira, H. J. Kimble, and K. C. Peng, Realization of the Einstein-Podolsky-Rosen Paradox for Continuous Variables, Phys. Rev. Lett. **68**, 3663 (1992).
[20] M. D. Reid, P. D. Drummond, W. P. Bowen, E. G. Cavalcanti, P. K. Lam, H. A. Bachor, U. L. Andersen, and G. Leuchs, Colloquium: The Einstein-Podolsky-Rosen paradox: From concepts to applications, Rev. Mod. Phys. **81**, 1727 (2009).
[21] S. L. W. Midgley, A. J. Ferris, and M. K. Olsen, Asymmetric Gaussian steering: When Alice and Bob disagree, Phys. Rev. A **81**, 022101 (2010).
[22] M. K. Olsen and J. F. Corney, Non-Gaussian continuous-variable entanglement and steering, Phys. Rev. A **87**, 033839 (2013).
[23] Q. Y. He and Z. Ficek, Einstein-Podolsky-Rosen paradox and quantum steering in a three-mode optomechanical system, Phys. Rev. A **89**, 022332 (2014).
[24] E. G. Cavalcanti, Q. Y. He, M. D. Reid, and H. M. Wiseman, Unified criteria for multipartite quantum nonlocality, Phys. Rev. A **84**, 032115 (2011).
[25] Q. Y. He and M. D. Reid, Genuine Multipartite Einstein-Podolsky-Rosen Steering, Phys. Rev. Lett. **111**, 250403 (2013).
[26] Q. Y. He, L. Rosales-Zárate, G. Adesso, and M. D. Reid, Secure Continuous Variable Teleportation and Einstein-Podolsky-Rosen Steering, Phys. Rev. Lett. **115**, 180502 (2015).
[27] I. Kogias, A. R. Lee, S. Ragy, and G. Adesso, Quantification of Gaussian Quantum Steering, Phys. Rev. Lett. **114**, 060403 (2015).
[28] V. Händchen, T. Eberle, S. Steinlechner, A. Samblowski, T. Franz, R. F. Werner, and R. Schnabel, Observation of one-way Einstein-Podolsky-Rosen steering, Nat. Photon. **6**, 596 (2012).
[29] S. Armstrong, M. Wang, R. Y. Teh, Q. H. Gong, Q. Y. He, J. Janousek, H. A. Bachor, M. D. Reid, and P. K. Lam, Multipartite Einstein-Podolsky-Rosen steering and genuine tripartite entanglement with optical networks, Nat. Phys. **11**, 167 (2015).
[30] M. D. Reid, Demonstration of the Einstein-Podolsky-Rosen paradox using nondegenerate parametric amplification, Phys. Rev. A **40**, 913 (1989).
[31] L. Rosales-Zárate, R. Y. Teh, S. Kiesewetter, A. Brolis, K. Ng, and M. D. Reid, Decoherence of Einstein–Podolsky–Rosen steering, J. Opt. Soc. Am. B **32**, A82 (2015).
[32] M. K. Olsen, Controlled Asymmetry of Einstein-Podolsky-Rosen Steering with an Injected Nondegenerate Optical Parametric Oscillator, Phys. Rev. Lett. **119**, 160501 (2017).
[33] M. K. Olsen, Entanglement and asymmetric steering over two octaves of frequency difference, Phys. Rev. A **96**, 063839 (2017).
[34] M. K. Olsen, Third-harmonic entanglement and Einstein-Podolsky-Rosen steering over a frequency range of more than an octave, Phys. Rev. A **97**, 033820 (2018).
[35] N. Tischler, F. Ghafari, T. J. Baker, S. Slussarenko, R. B. Patel, M. M. Weston, S. Wollmann, L. K. Shalm, V. B. Verma, S. W. Nam, H. C. Nguyen, H. M. Wiseman, and G. J. Pryde, Conclusive Experimental Demonstration of One-Way Einstein-Podolsky-Rosen Steering, Phys. Rev. Lett. **121**, 100401 (2018).
[36] X. Y. Huang, E. Zeuthen, Q. H. Gong, and Q. Y. He, Engineering asymmetric steady-state Einstein-Podolsky-Rosen steering in macroscopic hybrid systems, Phys. Rev. A **100**, 012318 (2019).
[37] L. Wang, S. C. Lv, and J. T. Jing, Quantum steering in cascaded four-wave mixing processes, Opt. Express **25**, 17457 (2017).
[38] Y. Liu, Y. Cai, Y. Xiang, F. Li, Y. P. Zhang, and Q. Y. He, Tripartite Einstein-Podolsky-Rosen steering with linear and nonlinear

beamsplitters in four-wave mixing of Rubidium atoms, Opt. Express **27**, 33070 (2019).

[39] Y. Liu, S. L. Liang, G. R. Jin, and Y. B. Yu, Genuine tripartite Einstein-Podolsky-Rosen steering in the cascaded nonlinear processes of third-harmonic generation, Opt. Express **28**, 2722 (2020).

[40] Y. Liu, S. L. Liang, G. R. Jin, Y. B. Yu, J. Y. Lan, X. B. He, and K. X. Guo, Generation of tripartite Einstein-Podolsky-Rosen steering by cascaded nonlinear process, Chin. Phys. B **29**, 050301 (2020).

[41] M. Piani and J. Watrous, Necessary and Sufficient Quantum Information Characterization of Einstein-Podolsky-Rosen Steering, Phys. Rev. Lett. **114**, 060404 (2015).

[42] M. Fadel, L. Ares, A. Luis, and Q. Y. He, Number-phase entanglement and Einstein-Podolsky-Rosen steering, Phys. Rev. A **101**, 052117 (2020).

[43] Y. Xiang, Y. Liu, Y. Cai, F. Li, Y. P. Zhang, and Q. Y. He, Monogamy relations within quadripartite Einstein-Podolsky-Rosen steering based on cascaded four-wave mixing processes, Phys. Rev. A **101**, 053834 (2020).

[44] J. Guo, H. X. Zou, Z. H. Zhai, J. X. Zhang, and J. R. Gao, Generation of continuous-variable tripartite entanglement using cascaded nonlinearities, Phys. Rev. A **71**, 034305 (2005).

[45] Y. B. Yu, Z. D. Xie, X. Q. Yu, H. X. Li, P. Xu, H. M. Yao, and S. N. Zhu, Generation of three-mode continuous-variable entanglement by cascaded nonlinear interactions in a quasiperiodic superlattice, Phys. Rev. A **74**, 042332 (2006).

[46] C. Pennarun, A. S. Bradley, and M. K. Olsen, Tripartite entanglement and threshold properties of coupled intracavity down-conversion and sum-frequency generation, Phys. Rev. A **76**, 063812 (2007).

[47] Y. B. Yu, F. M. Ji, Z. T. Shi, H. J. Wang, J. W. Zhao, and Y. J. Wang, Three-color entanglement generated by single-pass cascaded sum-frequency processes, Laser Phys. Lett. **14**, 035202 (2017).

[48] P. D. Drummond and C. W. Gardiner, Generalised P-representations in quantum optics, J. Phys. A **13**, 2353 (1980).

[49] C. W. Gardiner and P. Zoller, *Quantum Noise* (Springer-Verlag, Heidelberg, 2000).

[50] S. N. Zhu, Y. Y. Zhu, and N. B. Ming, Quasi-phase-matched third-harmonic generation in a quasi-periodic optical superlattice, Science **278**, 843 (1997).

[51] Y. Du, S. N. Zhu, Y. Y. Zhu, P. Xu, C. Zhang, Y. B. Chen, Z. W. Liu, N. B. Ming, X. R. Zhang, F. F. Zhang, and S. Y. Zhang, Parametric and cascaded parametric interactions in a quasiperiodic optical superlattice, Appl. Phys. Lett. **81**, 1573 (2002).

[52] Z. D. Gao, S. N. Zhu, S. Y. Tu, and A. H. Kung, Monolithic red-green-blue laser light source based on cascaded wavelength conversion in periodically poled stoichiometric lithium tantalate, Appl. Phys. Lett. **89**, 181101 (2006).

[53] A. Ferraro, M. G. A. Paris, M. Bondani, A. Allevi, E. Puddu, and A. Andreoni, Three-mode entanglement by interlinked nonlinear interactions in optical $\chi^{(2)}$ media, J. Opt. Soc. Am. B **21**, 1241 (2004).

[54] R. J. Glarber, Coherent and incoherent states of the radiation field, Phys. Rev. **131**, 2766 (1963).

[55] E. C. G. Sudarshan, Equivalence of Semiclassical and Quantum Mechanical Descriptions of Statistical Light Beams, Phys. Rev. Lett. **10**, 277 (1963).

[56] D. F. Walls and G. J. Milburn, *Quantum Optics* (Springer, Berlin, 1995).

[57] M. J. Collett and C. W. Gardiner, Squeezing of intracavity and traveling-wave light fields produced in parametric amplification, Phys. Rev. A **30**, 1386 (1984).

[58] A. S. Coelho, F. A. S. Barbosa, K. N. Cassemiro, A. S. Villar, M. Martinelli, and P. Nussenzveig, Three-color entanglement, Science **326**, 823 (2009).